

High Resolution X-ray Spectroscopy of G292.0+1.8/MSH 11-54

Jacco Vink,^{* a b} Johan Bleeker^b, Jelle S. Kaastra^b, Andrew Rasmussen^a

^aColumbia Astrophysics Laboratory, Columbia University, New York, NY, USA

^bSRON National Institute for Space Research, Sorbonnelaan 2, 3584 CA, Utrecht, Netherlands

We present a preliminary analysis of *XMM-Newton* observations of the oxygen-rich supernova remnant G292.0+1.8 (MSH 11-54). Although the spatial extent of the remnant is $8'$ the bright central bar is narrow ($1-2'$) resulting in RGS spectra of a high spectral quality. This allows us to spectroscopically identify a cool, $kT_e = 0.3$ keV, and underionized component, resolve details of the Fe-L complex, and resolve the forbidden and resonant lines of the O VII triplet. We are also able to constrain the kinematics of the remnant using Ne IX as observed in the second order spectrum, and O VIII in the first order spectrum. We do not find evidence for O VII line shifts or Doppler broadening ($\sigma_v < 731$ km s⁻¹), but line broadening of the Ne X Ly α line seems to be present, corresponding to $\sigma_v \sim 1500$ km s⁻¹.

1. INTRODUCTION

G292.0+1.8 (MSH 11-54) belongs to the class of oxygen-rich supernova remnants, which are probably the products of core collapse supernovae of the most massive stars, i.e. a main sequence mass in excess of $\sim 20M_\odot$.² It has a size of $\sim 8'$ and its morphology is characterized by a filamentary X-ray structure, and a bar stretching from the central east to the west side. The nature of this bar is unclear, but may have something to do with a structure in the progenitor's circumstellar medium [1].

Recently it was discovered that a region of hard X-ray emission, east of the center, harbors a 135 ms radio/X-ray pulsar [2,3]. This is of special interest as it is likely that G292.0+1.8 is the remnant of a very massive star (30-40 M_\odot , [4]). Such massive stars are thought to give birth to black holes [5]. Surprisingly, there are only a few examples of shell type supernova remnants with pulsar wind nebulae inside.

Chandra observations of G292.0+1.8 have revealed substantial variations in abundances within the remnant [1,4], the most prominent X-ray lines being O, Ne, Mg, Si and S.

XMM-Newton observed G292.0+1.8 in August

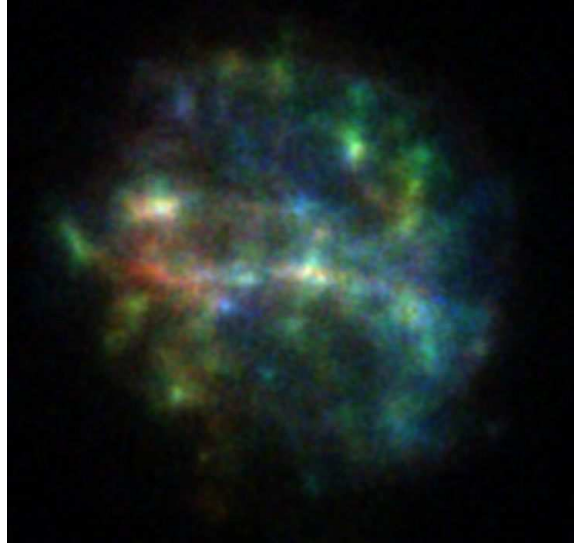


Figure 1. *XMM-Newton* EPIC-MOS image of G292.0+1.8. The RGB colors code for the line emission in O VIII, Mg XI, and Si XIII.

^{*}Chandra fellow

²See the review by Vink, these proceedings.

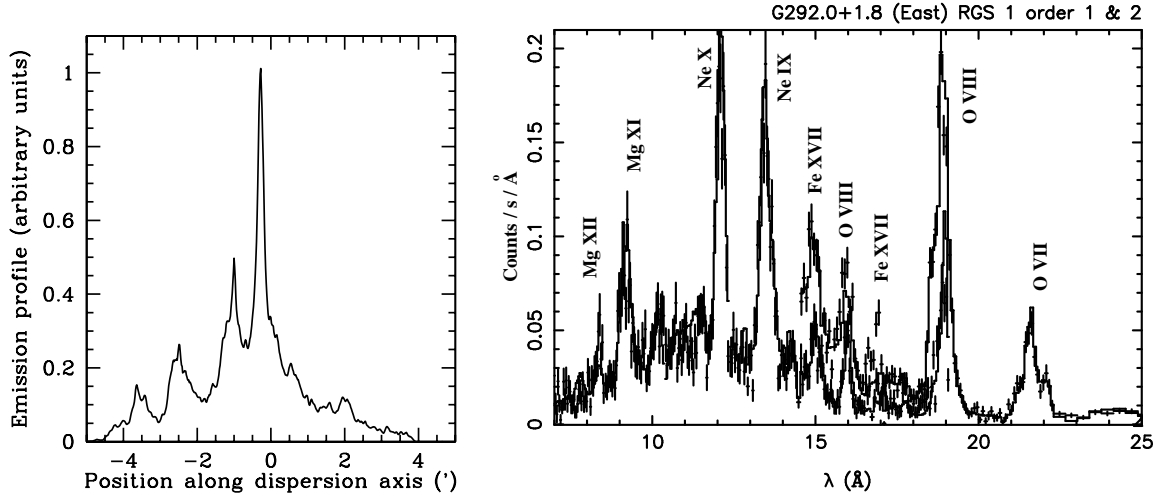


Figure 2. X-ray emission profile based on the high spatial resolution *Chandra* images, in the direction of the *XMM-Newton* RGS dispersion axis, using the O VII He α band (left). The sharp peak in the profile results in a high resolution *XMM-Newton* RGS spectrum (right).

2002, with a total observation time of ~ 28 ks. Here we report on a preliminary analysis of the data with an emphasis on the reflection grating spectrometer (RGS, [6]) data.

2. HIGH RESOLUTION SPECTROSCOPY

The peculiar bar-like feature across the remnant has an advantage for observation by the RGS instrument, as long as the dispersion axis is perpendicular to the bar, as was the case during this observation. As the RGS is a slitless spectrometer, the spectral resolution is degraded by the spatial extent of the observed object. The degradation is approximately 0.12 \AA per arcmin. However, the bar is bright with respect to the rest of the remnant and has a width of $1\text{--}2'$ (Fig. 2). The effective spectral resolution in FWHM is therefore $\sim 2 \text{ \AA}$. The relative spectral resolution increases at longer wavelengths. For shorter wavelengths higher resolution can be obtained by extracting second order spectra.

In order to perform a quantitative analysis of the RGS spectra the response matrix has to be

convolved with the spatial profile of the remnant (see [7,8]), for which we used the *Chandra*-ACIS images, which have a higher spatial resolution. The *Chandra* images were extracted in narrow energy bands in order to obtain the right profile for each element.

As can be seen in Fig. 2, the RGS spectrum reveals line features which are blended when observed with the *Chandra* or *XMM-Newton* CCD detectors (c.f. the spectra in [1]). The Fe XVII lines are of interest as they are weak and have not been resolved previously.

The spectral resolution is of sufficient quality in order to estimate the forbidden over resonant line ratios of the O VII He α triplet, which is an important plasma diagnostic [9]. The best fit with an absorption of $N_{\text{H}} = 4 \times 10^{21} \text{ cm}^{-2}$ gives a G-ratio of $(f + i/r) = 0.46 - 0.91$ (Fig. 3). According to the SPEX non-equilibrium ionization model, the triplet emission indicates a range for kT_e of $0.27 - 0.51 \text{ keV}$ (90% confidence).

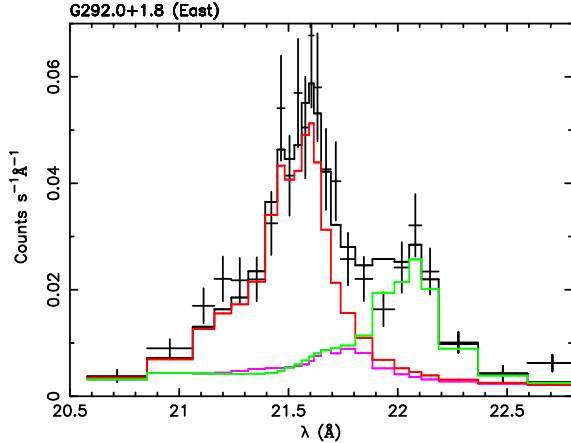


Figure 3. Detail of RGS 1 order 1 spectrum of the eastern region. It shows the decomposition of the O VII triplet in resonance (red), intercombination (magenta), and forbidden line emission (green).

3. A COOL COMPONENT

Previous X-ray studies of G292.0+1.8 typically found that the plasma temperature is $kT_e = 0.7$ keV, although an additional low 0.3 keV temperature component was found in a region near the rim of G292.0+1.8 [4]. However, fitting the RGS spectra with the SPEX non-equilibrium ionization model indicates that in addition to the 0.7 keV plasma component a much cooler component with $kT_e \sim 0.3$ keV has to be present throughout the remnant (see also the previous section). The spectral fits indicate that this component is also considerably more underionized than the 0.7 keV component: $n_{et} \leq 4 \times 10^{10} \text{ cm}^{-3} \text{ s}$ versus $n_{et} \sim 10^{11} \text{ cm}^{-3} \text{ s}$. The cool component varies in importance, with the contribution of the cool component to the total emission measure varying from 13% (in the west) to 28% (east). This component is the main source of the O VII emission shown in Fig. 2 and Fig. 3

4. THE KINEMATICS OF G292.0+1.8

In order to get a better idea of the ejected mass, the explosion energy, and the evolutionary phase of the G292.0+1.8, kinematical data are important, as the example of Cas A shows [10,11,12]. We are currently working on modeling the line profiles, and directly on the dispersed images in order to obtain kinematical information. This work is still in progress, but our preliminary results indicate that the O VII Ly α is coming from a plasma with no great bulk motions ($v < 114 \text{ km s}^{-1}$) and no apparent Doppler line broadening ($\sigma_v < 730 \text{ km s}^{-1}$, 95% confidence level). However, the Ne X Ly α emission, measured using the 2nd order spectra, is best fitted by including line broadening corresponding to $\sigma_v = 880 - 2880 \text{ km s}^{-1}$ (95% confidence range). Previous studies indicated that most of the Ne is associated with the ejecta, whereas the O emission has a large contribution from shock heated interstellar/circumstellar material. Our results therefore suggests that the blastwave has decelerated considerably, whereas at least some of the ejecta, presumably the material in relatively dense knots, are still moving with a high velocity.

5. CONCLUSIONS

We have presented preliminary results of an analysis of *XMM-Newton* observations of G292.0+1.8. We hope to improve on this analysis in the near future. The tentative conclusions are:

- It is possible to obtain high resolution RGS spectra from a relatively large object as G292.0+1.8, provided that narrow, outstanding features exist in the spatial emission profile along the dispersion axis.
- The RGS spectra of G292.0+1.8 indicate the presence of at least two temperature components, with $kT_e \sim 0.7$ keV and, somewhat unexpectedly, $kT_e \sim 0.3$ keV. The coolest component is needed in order to account for the observed O VII line emission.
- No significant line broadening (temperature of the shell) is indicated by the O VIII Ly α (0.65 keV) line emission: $\sigma_E < 1.4 \text{ eV}$

($< 731 \text{ km s}^{-1}$) (95% confidence), but significant line broadening seems to be present for the Ne X Ly α emission, corresponding to a velocity dispersion of $\sigma_v \sim 1500 \text{ km s}^{-1}$.

This work was supported by NASA's Chandra Postdoctoral Fellowship Award Nr. PF0-10011 issued by the Chandra X-ray Observatory Center, which is operated by the SAO under NASA contract NAS8-39073. This work is based on observations obtained with *XMM-Newton*, an ESA science mission, funded by its member states and the NASA (USA). SRON is financially supported by NWO, the Netherlands Organization for Scientific Research.

REFERENCES

1. S. Park et al., ApJL 564 (2002) L39.
2. F. Camilo et al., ApJL 567 (2002) L71.
3. J.P. Hughes et al., ApJL 591 (2003) L139.
4. M. Gonzalez and S. Safi-Harb, ApJL 583 (2003) L91.
5. A. Heger et al., ApJ 591 (2003) 288.
6. J.W. den Herder et al., A&A 365 (2001) L7.
7. A.P. Rasmussen et al., A&A 365 (2001) L231.
8. J. Vink et al., ApJL 587 (2003) 31.
9. D. Porquet et al., A&A 376 (2001) 1113.
10. J. Vink et al., A&A 339 (1998) 201.
11. R. Willingale et al., A&A 381 (2002) 1039.
12. T. Delaney and L. Rudnick, ApJ 589 (2003) 818.